**Earthquakes and Structures**, *Vol. 16, No. 2 (2019) 197-208*
DOI: https://doi.org/10.12989/eas.2019.16.2.197


# Novel Hilbert spectrum-based seismic intensity parameters interrelated with structural damage

Magdalini Tyrtaiou[a] and Anaxagoras Elenas*

*Department of Civil Engineering, Institute of Structural Statics and Dynamics, Democritus University of Thrace, 67100 Xanthi, Greece*

*(Received December 16, 2018, Revised January 15, 2019, Accepted January 16, 2019)*

**Abstract.** The objective of this study is to propose new seismic intensity parameters based on the Hilbert spectrum and to associate them with the seismic damage potential. In recent years the assessment of even more seismic features derived from the seismic acceleration time-histories was associated with the structural damage. For a better insight into the complex seismic acceleration time-history, Hilbert-Huang Transform (HHT) analysis is utilized for its processing, and the Hilbert spectrum is obtained. New proposed seismic intensity parameters based on the Hilbert spectrum are derived. The aim is to achieve a significant estimation of the seismic damage potential on structures from the proposed new intensity parameters confirmed by statistical methods. Park-Ang overall structural damage index is used to describe the postseismic damage status of structures. Thus, a set of recorded seismic accelerograms from all over the word is applied on a reinforced concrete frame structure, and the Park-Ang indices through nonlinear dynamic analysis are provided and considered subsequently as reference numerical values. Conventional seismic parameters, with well-known seismic structural damage interrelation, are evaluated for the same set of excitations. Statistical procedures, namely correlation study and multilinear regression analysis, are applied on the set of the conventional parameters and the set of proposed new parameters separately, to confirm their interrelation with the seismic structural damage. The regression models are used for the evaluation of the structural damage indices for every set of parameters, respectively. The predicted numerical values of the structural damage indices evaluated from the two sets of seismic intensity parameters are inter-compared with the reference values. The numerical results confirm the ability of the proposed Hilbert spectrum based new seismic intensity parameters to approximate the postseismic structural damage with a smaller Standard Error of Estimation than this accomplished of the conventional ones.

**Keywords:** seismic intensity parameters; Hilbert-Huang Transform (HHT); Park and Ang damage index; multilinear regression analysis; structural damage evaluation

## 1. Introduction

Earthquake excitations often lead to stiffness and strength deterioration of a structure causing permanent damage to the elements or the whole structure. The knowledge of the postseismic damage status in buildings is essential for their postseismic structural behavior and constitutes a wide range of current research (Kostinakis and Morfidis 2017).

In the literature of earthquake engineering research, many seismic intensity parameters are presented and associated with the grade of structural damage, described by different damage indices, as presented by several researchers (Cabãnas 1997, Elenas 1997, Elenas 2000, Elenas 2014, Vui and Hamid 2014). For the evaluation of all these parameters conventional accelerogram processing technics are utilized, which are meaningful only for stationary data. However, it is well-known that seismic accelerogram records are always nonstationary and nonlinear. The Hilbert-Huang Transform (HHT) analysis is a processing technique for nonstationary and nonlinear signals such as earthquake accelerograms (Huang *et al*. 1998, Huang *et al*. 1999, Huang *et al*. 2003, Long and Shen 2003, Zhang *et al*. 2003, Yan and Gao 2007). The HHT analysis decomposes the signal into a finite number of components, the intrinsic mode functions (IMFs), and presents the results as an amplitude-frequency-time function, the Hilbert spectrum.

In this study, new seismic intensity parameters are defined based on the Hilbert Spectrum. The conventional and the new parameters are evaluated for a set of seismic excitations and correlated with the structural damage, expressed by Park-Ang overall (global) structural damage index $DI_{PA,global}$ (Park and Ang 1987).

The multivariate correlation analysis is utilized for the assessment of the interrelationship between the dependent variable $DI_{PA,global}$ and the independent variables of conventional and new parameters. Subsequently, using the multilinear regression analysis (MLR), a prediction of the dependent variable $DI_{PA,global}$ is achieved using the set of the conventional and the set of the here new proposed parameters separately. The MLR analysis confirms the quite remarkable ability of new seismic parameters to predict the structural damage potential of an earthquake, while the extracted results seem to perform even better prediction than those achieved from the set of the conventional parameters.

*Corresponding author, Professor
E-mail: elenas@civil.duth.gr
[a]E-mail: mtyrtaio@civil.duth.gr



ISSN: 2092-7614 (Print), 2092-7622 (Online)

Table 1 Conventional seismic parameters

| Seismic Parameter | Reference |
|---|---|
| *PGA* | (Meskouris 2000) |
| *PGV* | (Meskouris 2000) |
| *PGD* | (Meskouris 2000) |
| *PGA/PGV* | (Meskouris *et al*. 1993) |
| *CP* | (Vanmarcke and Lai 1980) |
| $I_{Arias}$ | (Arias 1970) |
| $SMD_{TB}$ | (Trifunac and Brady 1975) |
| $P_{0.90}$ | (Jennings 1982) |
| $RMS_a$ | (Meskouris 2000) |
| $I_{FVF}$ | (Fajfar *et al*. 1990) |
| $SI_H$ | (Housner 1952) |
| *CAV* | (Cabãnas *et al*. 1997) |
| $DP_{AS}$ | (Araya and Saragoni 1984) |
| *SD* | (Chopra 1995) |
| *SV* | (Chopra 1995) |
| *SA* | (Chopra 1995) |
| $E_{inp}$ | (Uang and Bertero 1990) |
| $SI_K$ | (Kappos 1990) |
| $SI_{MR}$ | (Martinez and Rueda 1998) |
| *EPA* | (ATC 3-06 1978) |
| $EPA_{max}$ | (ATC 3-06 1978) |

## 2. Conventional seismic intensity parameters

As aforementioned many seismic intensity parameters have been defined that play a significant role in the assessment of seismic damage potential (Ercan *et al*. 2017, Kostinakis 2018).

Several well-known and extensively used seismic intensity parameters have been utilized in this study. Thus, the following conventional seismic parameters are considered: peak ground acceleration (*PGA*); peak ground velocity (*PGV*); peak ground displacement (*PGD*); the ratio *PGA/PGV*; central period (*CP*); Arias intensity ($I_{Arias}$); strong motion duration of Trifunac-Brady ($SMD_{TB}$); seismic power ($P_{0.90}$); root mean square acceleration ($RMS_a$); seismic intensity of Fajfar-Vidic-Fischinger ($I_{FVF}$); Housner's spectrum intensity ($SI_H$); cumulative absolute velocity (*CAV*); seismic destructiveness potential of Araya-Saragoni ($DP_{AS}$); spectral displacement (*SD*); spectral velocity (*SV*); spectral acceleration (*SA*); seismic absolute input energy ($E_{inp}$); Kappos spectrum intensity ($SI_K$); spectrum intensity of Martinez-Rueda ($SI_{MR}$) and effective peak acceleration (*EPA*). Table 1 shows all the utilized parameters and the literature references that contain their definitions.

## 3. The Hilbert-Huang Transform (HHT)

In nature physical processes give us data that are most likely to be both nonlinear and nonstationary. The HHT is a time-frequency analysis technique that offers higher frequency resolution and more accurate timing of transient and non-stationary signal events than other more common techniques for the analysis of nonlinear signals (e.g., Fourier transform, wavelet analysis) which assume that signals are stationary, at least within the time window of observation.

The HHT was presented first by Huang *et al*. (1998) and consists of two parts: the empirical mode decomposition (EMD) and the Hilbert spectral analysis (HSA).

### 3.1 Empirical Mode Decomposition (EMD)

The EMD decompose complicated signal data into oscillatory modes, and each of them represents an intrinsic mode function (IMF) which per definition satisfies the following two requirements:

1. In the whole seismic signal, the number of extrema and zero-crossings must be either equal or differ at most by one.
2. At any point, the mean value of the envelope defined by the local maxima and the envelope defined by the local minima is zero.

Considering the above definition, we carry out the following procedure. For a seismic signal $X(t)$, all the local extremes must be identified and connected by a cubic spline to create the upper envelope of the signal $u_{\max}(t)$ An identical procedure is performed for the local minima to create the lower envelope of the signal $u_{\min}(t)$. The two envelopes must enclose the whole signal between them. The mean value of the two envelopes assigned as $m_1(t)$ is provided in Eq. (1).

$$m_1(t) = \frac{\left(u_{max}(t) - u_{min}(t)\right)}{2} \quad (1)$$

The difference between the seismic signal and the $m_1(t)$ is the first component $h_1(t)$ as given in Eq. (2).

$$h_1(t) = X(t) - m_1\ (t) \quad (2)$$

Going on the procedure, the term $h_1(t)$ is considered to be the signal, and thus

$$h_{11}(t) = h_1(t) - m_{11}(t) \quad (3)$$

where $m_{11}(t)$ is the new mean of the upper and lower envelopes of $h_1(t)$, this process is repeated for $k$-times, and $h_{1k}(t)$ is given by Eq. (4).

$$h_{1k}(t) = h_{1(k-1)}\ (t) - m_{1k}(t) \quad (4)$$

The $h_{1k}(t)$=$c_1(t)$ is the first IMF and contains the shortest period of the signal. Afterward, the residue $r_1(t)$ is obtained by subtracting the first IMF from the initial signal.

$$r_1(t) = X(t) - c_1(t) \quad (5)$$

The residue $r_1(t)$ contains components of longer periods and is subsequently considered as new data. The new data are submitted to the same sifting procedure as mentioned until all the $r_j(t)$ functions are obtained (Eq. (6)).

$$r_j(t) = r_{(j-1)}(t) - c_j(t), \qquad j = 2, 3, \ldots, n \quad (6)$$

The iteration process stops when one of the two following criteria is true:

• The component $c_n(t)$ or the residue $r_n(t)$ is less than a predetermined value.

• The residue $r_n(t)$ is a monotonic function and, therefore, no further IMFs can be extracted from it.

At the end of the procedure, the initial seismic signal

$X(t)$ is the sum of all IMFs and the residue $r_n(t)$, which can be a monotonic mean trend, a curve with only one extreme, or a constant function (Eq. (7)).

$$X(t) = \sum_{J=1}^{n} c_j\,(t) + r_n\,(t) \tag{7}$$

### *3.2 Hilbert Spectral Analysis (HSA)*

During HSA the Hilbert transform is applied to each intrinsic mode function (IMF) $c_j(t)$, as shown in Eq. (8).

$$y_j(t) = \frac{1}{\pi}\, PV \int_{-\infty}^{\infty} \frac{c_j(\tau)}{t-\tau}\, d\tau \tag{8}$$

Where *PV* indicates the Cauchy principal value of the integral. The IMF $c_j(t)$ and the Hilbert transform $y_j(t)$ form an analytical signal $z_j(t)$ as presented in Eq. (9).

$$z_j(t)=c_j(t)+iy_j(t)=a_j(t)e^{i\theta_j(t)} \tag{9}$$

Where $a_j(t)$ is the amplitude and $\theta_j(t)$ is the phase function. These quantities are defined in Eqs. (10) and (11).

$$a_j(t) = \sqrt{c_j^2(t) + y_j^2(t)} \tag{10}$$

$$\theta_j(t) = \arctan\left(\frac{y_j(t)}{c_j(t)}\right) \tag{11}$$

The instantaneous angular velocity $\omega(t)$ of the rotation is defined as the derivative of phase function, from which the instantaneous frequency $f_j(t)$ is calculated (Eq. (12)).

$$\omega_j(t) = \frac{d\theta_j(t)}{dt} = 2\pi \cdot f_j(t) \tag{12}$$

Using the Eqs. (10)-(12) the IMF components can be defined Eq. (13).

$$c_j(t) = \mathrm{Re}(a_j(t)e^{i\theta_j(t)}) = a_j(t)cos\theta_j(t) \tag{13}$$

Where Re() denotes the real part of the analytical signal $z_j(t)$. Thus, the initial signal can be written as

$$X(t) = \mathrm{Re}\ \left[\sum_{j=1}^{n} a_j(t)\cos(\int 2\pi \cdot f_j(t)dt)\right] \tag{14}$$

In Eq. (14), the residue $r_n(t)$ is not included because it is either a monotonic or a constant function. Thus, the amplitude and frequency can be expressed as functions of time in a three-dimensional plot and can form the time-frequency distribution of the amplitude. This time-frequency amplitude distribution is called the Hilbert amplitude spectrum (Fig. 1), *HS* (*f*, *t*), or merely Hilbert spectrum (Alvanitopoulos *et al*. 2010, 2012, Vrochidou *et al*. 2016, 2018).

## 4. Proposed new seismic parameters

Every Hilbert spectrum which presents the distribution of time-frequency-amplitude leads to a time-frequency-energy (square of amplitude) description of a signal. From the illustrated Hilbert spectrum plot, the volume of the confined space is evaluated. The numerical value of the volume limited from every produced Hilbert spectrum of

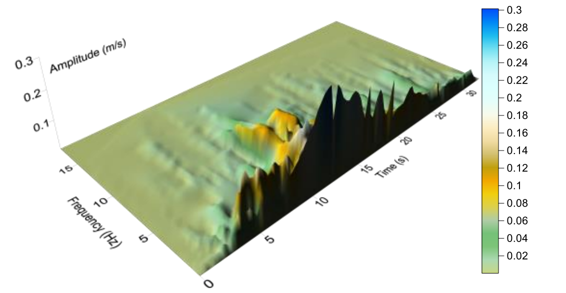


(a) The seismic event “Tabas H1” (16/09/1978)

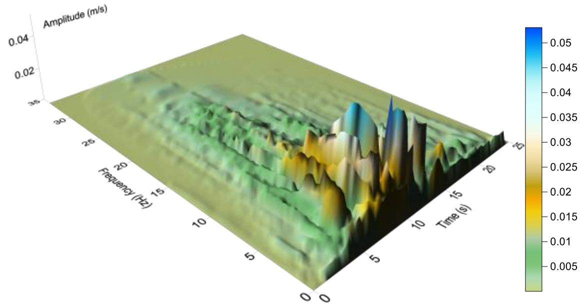


(b) The seismic event “Loma Prieta H1” (18/10/1989)

Fig. 1 Hilbert Spectrum of two seismic excitations

seismic velocity consists an essential seismic feature because it reveals the amount of the released energy during the seismic excitation of the considered record. For this research, the specific volume is considered as a new seismic parameter which is denoted as $V_{HHT}$ and is defined in Eq. (15).

$$V_{HHT} = \int_0^{f_{max}} \int_0^{t_{max}} a(f,t) \cdot df \cdot dt \tag{15}$$

Where $a(f, t)$ denotes the instantaneous amplitude.

For example, for the earthquake “Tabas H1” the biggest part of the energy is released during 10 s and 20 s while for the earthquake “Loma Prieta H1” the most significant part of the energy is released during 5 s and 15 s of its duration where the volume obtained from the Hilbert spectrum is increased as observed in Fig. 2(b).

From the values of the instantaneous amplitude $a_i$, that are obtained from the analytical signal, the maximum and the mean value are distinguished and considered as new seismic intensity parameters which are presented as

$$A_{max,HHT} = max(\alpha(f,t)) \tag{16}$$

$$A_{mean,HHT} = mean(\alpha(f,t)) \tag{17}$$

and

$$A_{dif,HHT} = A_{\max,HHT} - A_{mean,HHT} \tag{18}$$

The upper surface of the defined volume obtained from every Hilbert spectrum (see Fig. 1) is presented as an additional new parameter and described as

$$S_{HHT} = \int_0^{f_{max}} \int_0^{t_{max}} \sqrt{1 + \left(\frac{da(f,t)}{df}\right)^2 + \left(\frac{da(f,t)}{dt}\right)^2} \cdot df \cdot dt \tag{19}$$

The surface $S_{HHT}$ is interrelated with the instantaneous

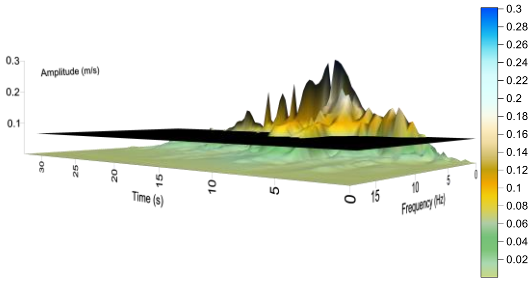


(a) The seismic event "Tabas H1" (16/09/1978)

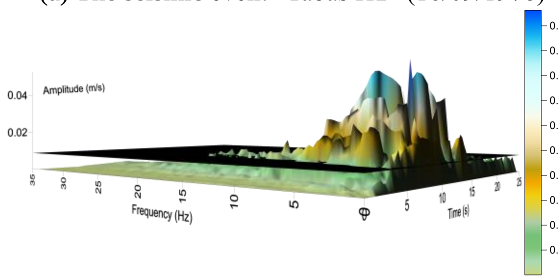


(b) The seismic event "Loma Prieta H1" (18/10/1989)

Fig. 2 A layer crosses the amplitude-axis of Hilbert spectrum vertically at $A_{mean,HHT}$ point

frequency, the instantaneous amplitude, consequently is interrelated with the velocity that corresponds to every instantaneous frequency of the signal.

Subsequently, a parallel layer to the time-frequency one is set, which intersects the $z$-axis (axis of $A_{mean,HHT}$ amplitudes) of the Hilbert spectrum at the point of $A_{mean,HHT}$ value (see Fig. 2) and the volume over and under the placed $A_{mean,HHT}$-layer and the corresponding upper surface of the defined space over the specific layer are evaluated. These values are denoted respectively as

$$V_{Pos,HHT} = \int_0^{f_{max}} \int_0^{t_{max}} a(f,t) \cdot df \cdot dt \quad a \geq a_{mean} \tag{20}$$

$$V_{Neg,HHT} = \int_0^{f_{max}} \int_0^{t_{max}} a(f,t) \cdot df \cdot dt \quad a < a_{mean} \tag{21}$$

and

$$S_{Pos,HHT} = \int_0^{f_{max}} \int_0^{t_{max}} \sqrt{1 + \left(\frac{da(f,t)}{df}\right)^2 + \left(\frac{da(f,t)}{dt}\right)^2} \cdot df \cdot dt \tag{22}$$

$$here \ a \geq a_{mean}$$

In addition, the following new quantities are defined in Eqs. (23)-(26).

$$VA_{max,HHT} = V_{HHT} \cdot A_{max,HHT} \tag{23}$$

$$VA_{mean,HHT} = V_{HHT} \cdot A_{mean,HHT} \tag{24}$$

$$VA_{dif,HHT} = V_{HHT} \cdot \left(A_{max,HHT} - A_{mean,HHT}\right) \tag{25}$$

$$A_{Pos,HHT} = \frac{V_{Pos,HHT}}{S_{Pos,HHT}} \tag{26}$$

Where the volume $V_{HHT}$ obtained from the Hilbert spectrum is increased while is multiplied by the maximum and mean amplitude and their difference. The quantities, $VA_{max,HHT}$, $VA_{mean,HHT}$, $VA_{dif,HHT}$, are three new quantities which are representative of every seismic record since every one of them includes two or three characteristic features of each record. In the case where the difference between the mean and maximum amplitude is minimal the quantity $VA_{dif,HHT}$ is statistically equivalent to one of the other two quantities.

Finally, the volume $V_{Pos,HHT}$ is divided by the $S_{Pos,HHT}$, and new parameter $A_{Pos,HHT}$ is obtained, which can be considered as the mean amplitude of the positive volume (volume above the $A_{mean,HHT}$ -layer) of the Hilbert spectrum.

## 5. Park-Ang structural damage index

For the assessment of the seismic damage potential, the structural damage is quantified by a single numerical value named "damage index" (DI) and correlated with seismic parameters (Elenas and Meskouris 2001, Nanos *et al.* 2008). In this study, the global structural DI of Park-Ang is used (Park and Ang 1985, Park *et al.* 1987). It is an index expressed by the response of a structure during a seismic excitation evaluated by nonlinear dynamic analysis. Consistent with the dynamic behavior, this index expresses the seismic structural damage as a linear combination of the damage caused by excessive deformation and that contributed by repeated cyclic loading effect. First, the Park-Ang damage index $DI_{PA,local}$ is defined locally for each element according to the following equation.

$$DI_{PA,local} = \frac{\theta_m - \theta_r}{\theta_u - \theta_r} + \frac{\beta}{M_y \theta_u} E_h \tag{27}$$

Where $\theta_m$ is the maximum rotation during the loading history, $\theta_u$ is the ultimate rotation capacity of the section, $\theta_r$ is the recoverable rotation at unloading, $\beta$ is a constant parameter (0.1-0.15 for nominal strength deterioration (Reinhorn *et al*. 2009), $M_y$ is the yield moment of the section, and $E_h$ is the dissipated hysteretic energy in the section.

The global damage is obtained as a weighted average of the local one at the ends of each element, with the dissipated energy as the weighting function as shown in Eq. (28).

$$DI_{PA,global} = \frac{\sum_{i=1}^{n} DI_{PA,local} \cdot E_i}{\sum_{i=1}^{n} E_i} \tag{28}$$

Where $E_i$ is the energy dissipated at location $i$ and $n$ is the number of locations at which the local damage is calculated. Under elastic response, the value of $DI_{PA,global}$ is equal zero while $DI_{PA,global} \geq 1.0$ signifies complete collapse or total damage of the structure.

## 6. Application

### *6.1 Seismic excitations*

Two sets, of total 80 natural seismic excitations are studied in this paper, and the association of the destructive power of an earthquake with the caused damage on the

Table 2 Number of excitations employed per country

| Country | Number of accelerograms |
|---|---|
| Albania | 1 |
| Armenia | 1 |
| California | 14 |
| Canada | 2 |
| France | 2 |
| Iceland | 2 |
| Iran | 9 |
| Italy | 11 |
| Japan | 6 |
| Mexico | 2 |
| New Zealand | 7 |
| San Salvador | 1 |
| Turkey | 19 |
| Uzbekistan | 3 |
| Albania | 1 |

Table 3 Number of excitations employed per *PGA* range

| PGA Range (g) | Number of accelerograms |
|---|---|
| 0.01-0.1 | 7 |
| 0.1-0.2 | 17 |
| 0.2-0.3 | 10 |
| 0.3-0.4 | 9 |
| 0.4-0.5 | 5 |
| 0.5-0.6 | 4 |
| 0.6-0.7 | 5 |
| 0.7-0.8 | 5 |
| 0.8-0.9 | 7 |
| > 0.9 | 11 |

Table 4 Number of excitations employed per magnitude

| Magnitude (Richter) | Number of accelerograms |
|---|---|
| 4-5 | 1 |
| 5-6 | 10 |
| 6-7 | 42 |
| 7-8 | 27 |

Table 5 Statistical results of conventional seismic parameters

| Statistics | $PGA$ (m/s$^2$) | $PGV$ (m/s) | $PGD$ (m) |
|---|---|---|---|
| Min value | 0.304 | 0.030 | 0.003 |
| Max value | 13.615 | 1.152 | 4.341 |
| Mean value | 4.541 | 0.352 | 0.290 |
| Stand. Dev. | 3.446 | 0.251 | 0.713 |
| Statistics | $PGA/PGV$ (g·s /m) | $CP$ (s) | $I_{Arias}$ (m/s) |
| Min value | 0.314 | 0.052 | 0.015 |
| Max value | 3.248 | 0.802 | 17.041 |
| Mean value | 1.420 | 0.223 | 2.823 |
| Stand. Dev. | 0.687 | 0.125 | 3.551 |
| Statistics | $SMD_{TB}$ (s) | $P_{0.90}$ (m$^2$/s$^4$) | $RMS_a$ (m/s$^2$) |
| Min value | 2.080 | 0.005 | 0.038 |
| Max value | 39.100 | 7.442 | 1.636 |
| Mean value | 15.203 | 1.740 | 0.533 |
| Stand. Dev. | 16.150 | 2.037 | 0.393 |
| Statistics | $I_{FVF}$ (m·s$^{-3/4}$) | $SI_H$ (m) | $CAV$ (g·s) |
| Min value | 0.041 | 0.096 | 0.058 |
| Max value | 2.095 | 5.082 | 4.652 |
| Mean value | 0.633 | 1.432 | 1.214 |
| Stand. Dev. | 0.462 | 1.153 | 1.009 |
| Statistics | $DP_{AS}$ (m·s) | $SD$ (m) | $SV$ (m/s) |
| Min value | 0.000 | 0.006 | 0.051 |
| Max value | 0.226 | 0.369 | 2.408 |
| Mean value | 0.032 | 0.083 | 0.599 |
| Stand. Dev. | 0.045 | 0.073 | 0.487 |
| Statistics | $SA$ (m/s$^2$) | $E_{inp}$ (m$^2$/s$^2$) | $SI_K$ (m) |
| Min value | 0.058 | 0.001 | 0.016 |
| Max value | 1.975 | 6.175 | 1.024 |
| Mean value | 0.653 | 0.690 | 0.259 |
| Stand. Dev. | 0.469 | 1.173 | 0.218 |
| Statistics | $SI_{MR}$ (m/s) | $EPA$ (g) | $EPA_{\max}$ (g) |
| Min value | 0.042 | 0.018 | 0.030 |
| Max value | 1.391 | 1.001 | 1.035 |
| Mean value | 0.466 | 0.360 | 0.387 |
| Stand. Dev. | 0.350 | 0.252 | 0.269 |

constructions is achieved (Elenas 1995, 2000). All the accelerograms represent natural seismic acceleration time series derived from ground strong motions all over the world, shown in Table 2. The utilized accelerograms generate a broad spectrum of damage (low, medium, large and total) for statistical reasons. Table 3 and Table 4 provides the number of excitations used per *PGA* range and Richter magnitude scale, respectively.

### 6.2 Evaluation of seismic parameters

At first, all the aforementioned seismic parameters are evaluated for every examined seismic excitation, and the results are presented in Table 5.

Accelerograms are complex signals that carry rich inherent information. After the calculation of the conventional seismic parameters, the Hilbert Huang transform (HHT) is applied at the velocity time series produced of the integrals of the 80 accelerograms considered. The HHT can generate earthquake signals that conserve the nonstationarity characteristics of a real seismic signal (Huang *et al.* 2003, Zhang *et al.* 2003). With the HHT the defined frequency of a signal is based on an adaptive basis, and the results are presented as an amplitude-frequency-time distribution, the Hilbert spectrum, for every excitation. For the calculation of the instantaneous frequencies $f_i$ and amplitudes $a_i$ of every utilized seismic excitation, where $i$ is the number of time locations, a code of the program MATLAB (Bradley *et al.* 2007) has been used, and the delivered Hilbert spectra are illustrated in graphs (Figs. 1-2).

All the proposed parameters are evaluated from the obtained Hilbert spectra, and their statistical values are presented in Table 6.

### 6.3 Reinforced concrete frame

Subsequently, all the accelerograms are applied to a seven-story reinforced concrete frame structure with a total height of 22 m. The examined structure is designed in agreement with the rules of the recent Eurocodes for structural concrete and aseismic structures, EC2 (2000) and

Table 6 Statistical values of the proposed new seismic parameters

| Statistics | $S_{HHT}$ (-) | $V_{HHT}$ (m/s) | $V_{Pos,HHT}$ (m/s) |
|---|---|---|---|
| Min value | 153.591 | 0.205 | 0.060 |
| Max value | 4062.689 | 69.376 | 7.393 |
| Mean value | 1185.912 | 6.422 | 1.303 |
| Stand. Dev. | 871.246 | 10.286 | 1.306 |
| Statistics | $V_{Neg,HHT}$ (m/s) | $S_{Pos,HHT}$ (-) | $A_{max,HHT}$ (m/s) |
| Min value | 0.000 | 0.387 | 0.011 |
| Max value | 68.461 | 313.910 | 7.475 |
| Mean value | 4.762 | 71.763 | 0.515 |
| Stand. Dev. | 9.824 | 67.229 | 1.245 |
| Statistics | $A_{mean,HHT}$ (m/s) | $A_{dif,HHT}$ (m/s) | $VA_{dif,HHT}$ (m$^2$/s$^2$) |
| Min value | 0.001 | 0.010 | 0.005 |
| Max value | 0.469 | 7.022 | 292.948 |
| Mean value | 0.046 | 0.470 | 12.544 |
| Stand. Dev. | 0.106 | 1.143 | 46.912 |
| Statistics | $VA_{max,HHT}$ (m$^2$/s$^2$) | $VA_{mean,HHT}$ (m$^2$/s$^2$) | $A_{Pos,HHT}$ (m/s) |
| Min value | 0.005 | 0.000 | 0.002 |
| Max value | 322.619 | 29.670 | 0.388 |
| Mean value | 13.789 | 1.245 | 0.038 |
| Stand. Dev. | 51.616 | 4.756 | 0.067 |

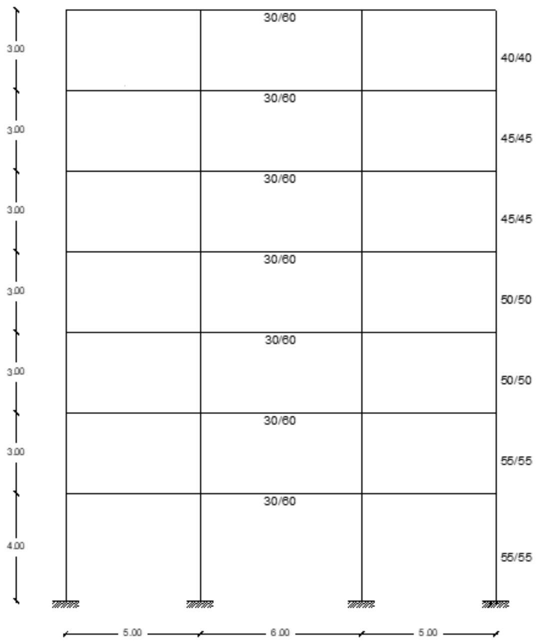


Fig. 3 Seven-story reinforced concrete frame

EC8 (2004) and shown in Fig. 3, where the dimensions are provided in meter and centimeter, respectively. The cross-section of the beams are *T*-shapes with 30 cm width, 20 cm plate thickness, 60 cm total beam height. The effective plate width is 1.15 m at the end-bays and 1.80 m at the middle-bay. The distance between frames in the three-dimensional structure has been chosen to be 6 m. The building has been considered as an “importance class II”, “ductility class Medium” and “subsoil of type B”.

Additionally, to the dead weight and the seismic loading, snow, wind and live loads have been taken into account. The fundamental period of the frame is 0.95 s. After the design procedure of the reinforced concrete frame

Table 7 Number of excitations employed per $DI_{PA,global}$ range

| $DI_{PA,global}$ | Number of accelerograms |
|---|---|
| 0.01-0.1 | 15 |
| 0.1-0.2 | 16 |
| 0.2-0.3 | 11 |
| 0.3-0.4 | 10 |
| 0.4-0.5 | 3 |
| 0.5-0.6 | 5 |
| 0.6-0.7 | 4 |
| 0.7-0.8 | 3 |
| 0.8-0.9 | 2 |
| > 0.9 | 11 |

structure, a non-linear dynamic analysis has been occurred using the software computer program IDARC (Reinhorn *et al.* 2009) for the evaluation of the structural seismic response for every seismic excitation utilized in the present study. The hysteretic behavior of beams and columns has been specified at both ends of each one using a three-parameter Park model.

This model incorporates stiffness degradation, strength deterioration, non-symmetric response, slip-lock, and a trilinear monotonic envelope. The parameter values, which specify the above degrading parameters, have been chosen from experimental results of cyclic force-deformation characteristics of typical components of studied structure (Park *et al.* 1987, Gholamreza and Elham 2018). Thus, the nominal parameters for stiffness degradation and strength deterioration have been chosen. In contrast, no pinching has been taken into account. From the derived response parameters of the nonlinear dynamic analysis, this paper concentrates on Park-Ang overall structural index ($DI_{PA,global}$). Table 7 presents the $DI_{PA,global}$ per number of excitations employed.

## 7. Multiple linear Regression (MLR) analysis of the results

Regression analyses are a set of statistical techniques that allow one to assess the relationship between one dependent variable (DV) and several independent variables (IVs). Regression techniques can be applied to a data set in which the IVs are correlated with one another and with the DV to varying degrees.

In multiple linear regression in which several IVs are combined to predict a value on a DV for each subject, the result of the regression represents the best prediction of a DV from several continuous (or dichotomous) IVs. The equation for the multilinear regression takes the following form

$$Y' = A + B_1 X_1 + B_2 X_2 + \ldots + B_k X_k \qquad (29)$$

where $Y'$ is the predicted value on the DV, $A$ is the $Y$-intercept (the value of $Y$ when all the $X$ values are zero), the $X_i$ represent the various IVs (of which there are $k$), and the $B_i$ ($i$=1, …, $k$) are the coefficients assigned to each of the

Table 8 Pearson and Rank correlation of conventional seismic parameters with $DI_{PA,global}$

| *a/a* | Parameter | Pearson Correlation with $DI_{PA,global}$ | Rank Correlation with $DI_{PA,global}$ |
|---|---|---|---|
| 1 | $PGA$ | 0.557 | 0.684 |
| 2 | $PGV$ | 0.592 | 0.906 |
| 3 | $PGD$ | 0.445 | 0.765 |
| 4 | $PGA/PGV$ | -0.445 | -0.483 |
| 5 | $CP$ | 0.088 | 0.299 |
| 6 | $I_{Arias}$ | 0.462 | 0.779 |
| 7 | $SMD_{TB}$ | 0.088 | 0.108 |
| 8 | $P_{0.90}$ | 0.590 | 0.720 |
| 9 | $RMS_a$ | 0.646 | 0.794 |
| 10 | $I_{FVF}$ | 0.561 | 0.927 |
| 11 | $SI_H$ | 0.589 | 0.906 |
| 12 | $CAV$ | 0.534 | 0.720 |
| 13 | $DP_{AS}$ | 0.461 | 0.781 |
| 14 | $SD$ | 0.688 | 0.933 |
| 15 | $SV$ | 0.650 | 0.911 |
| 16 | $SA$ | 0.640 | 0.786 |
| 17 | $E_{inp}$ | 0.436 | 0.904 |
| 18 | $SI_K$ | 0.685 | 0.920 |
| 19 | $SI_{MR}$ | 0.599 | 0.703 |
| 20 | $EPA$ | 0.693 | 0.723 |
| 21 | $EPA_{max}$ | 0.682 | 0.733 |

Table 9 Pearson and Rank correlation of new seismic parameters with $DI_{PA,global}$

| *a/a* | Parameter | Pearson Correlation with $DI_{PA,global}$ | Rank Correlation with $DI_{PA,global}$ |
|---|---|---|---|
| 1 | $S_{HHT}$ | -0.233 | -0.238 |
| 2 | $V_{HHT}$ | 0.530 | 0.766 |
| 3 | $V_{Pos,HHT}$ | 0.265 | 0.457 |
| 4 | $V_{Neg,HHT}$ | 0.417 | 0.823 |
| 5 | $S_{Pos,HHT}$ | -0.381 | -0.538 |
| 6 | $A_{max,HHT}$ | 0.560 | 0.898 |
| 7 | $A_{mean,HHT}$ | 0.605 | 0.879 |
| 8 | $A_{dif,HHT}$ | 0.554 | 0.885 |
| 9 | $VA_{dif,HHT}$ | 0.443 | 0.875 |
| 10 | $A_{Pos,HHT}$ | 0.637 | 0.935 |
| 11 | $VA_{mean,HHT}$ | 0.447 | 0.891 |
| 12 | $VA_{max,HHT}$ | 0.444 | 0.876 |

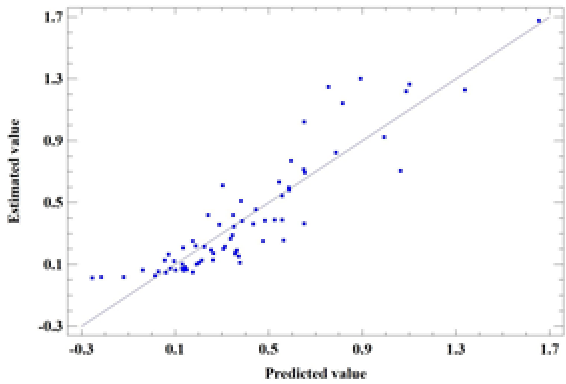


Fig. 4 Scatterplot estimated vs. predicted values of $DI_{PA,global}$ for Model 1

IVs during regression. Although the same intercept and coefficients are used to predict the values on the DV for all cases in the sample, a different $Y'$value is predicted for each subject as a result of inserting the subject's $X$ values into the equation. The goal of regression is to arrive at the set of $B$ values, called "regression coefficients", for the IVs that bring the $Y'$ values predicted from the equation as close as possible to the $Y$ values obtained by measurement.

In this research, the dependent variable DV is the Park-Ang overall structural damage index ($DI_{PA,global}$) and the seismic parameters are the independent variables (IVs). Correlation and regression analyses are utilized to validate both the ability of the proposed new intensity parameters to express their interrelation with the structural damage and to predict the damage grade, of at least the same quality in comparison with the conventional ones or even better.

The regression analysis first is applied to a data set in which the IVs are the conventional seismic parameters and second to a data set in which IVs are the new proposed seismic parameters. There are, however, some general considerations for choosing IVs. Regression will be best when each IV is strongly correlated with the DV but uncorrelated with other IVs. Then, a general goal of regression is to identify the fewest IVs necessary to predict a DV, where each IV predicts a substantial and independent segment of the variability in the DV.

In both cases is determined the correlation between the DV and both data sets of IVs (Pejovic *et al*. 2017). Initially, the interdependence between the studied parameters and the $DI_{PA,global}$ is investigated. A strong relationship between the $DI_{PA,global}$ and an IV is usually associated with the importance of the IV in the regression equation. Several correlation coefficients are measuring the degree of correlation between two variables. The most common of these is the Pearson correlation coefficient (multilinear regression usually refers to this), which is sensitive only to a linear relationship between two variables (which may be present even when one variable is a nonlinear function of the other). Other correlation coefficients have been developed to be more robust the Pearson correlation that is, more sensitive to nonlinear relationships. Although a strong relationship between the DV and IVs is requested a non-absolute straight linear relationship between the $DI_{PA,global}$ and IVs is a fact. For this reason, in this research, Rank correlation coefficients as alternatives to Pearson's coefficient, is used to prescribe the relationship between the variables with a coefficient less sensitive to non-normality in distributions.

The correlation between the variables is estimated by the software program STATGRAPHICS Centurion XVII (Statpoint Technologies Inc. 2016). In Table 8 of the correlation between the $DI_{PA,global}$ and the conventional seismic parameters is presented while Table 9 reveals the correlation between the $DI_{PA,global}$ and the new parameters. The numerical results show that the proposed new parameter reveal at least the same correlation degree with the conventional ones.

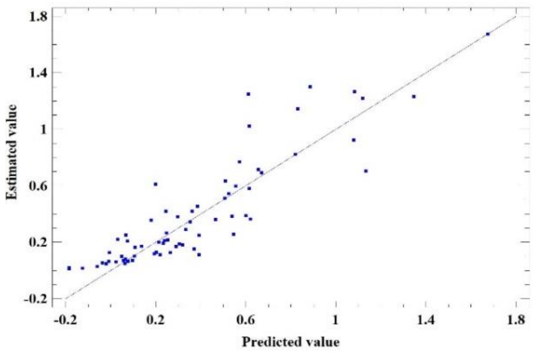


Fig. 5 Scatterplot estimated vs. predicted values of $DI_{PA,global}$ for Model 2

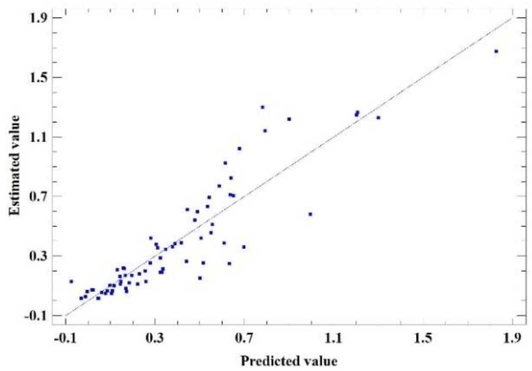


Fig. 6 Scatterplot estimated vs. predicted values of $DI_{PA,global}$ for Model 3

## 8. Created regression models

As aforementioned, multiple linear regression (MLR) is used to model the relationship between every set of explanatory variables (IVs) and the corresponding $DI_{PA,global}$ by fitting a linear equation to each couple of data set. The program STATGRAPHICS is also used to attain the regression analyses, and the best model with the fewest explanatory variables for every set of parameters is selected using the ordinary least square method. The procedure considers all possible regressions involving different combinations of the independent variables. It compares models based mainly on the Standard Error of Estimation (SEE), the Mean Squared Error (MSE) and the Adjusted $R$-Squared $(R^2)$. The best model considered the one with the fewest IVs, the smallest SEE and MSE and the highest $R^2$ and Adjusted $R^2$.

Eventually, the best constructed statistical models for each set of IVs for the training set of the velocity time-histories (integral of the acceleration time-histories) of the first 70 examined accelerograms shown in Table 1, are determined and presented below.

### *8.1 Model 1 and 2 for the set of conventional parameters as IVs.*

The best Models 1 and 2 for the first set of IVs contains a subset of 5 explanatory parameters with and without a constant term. The results of the regression analysis for

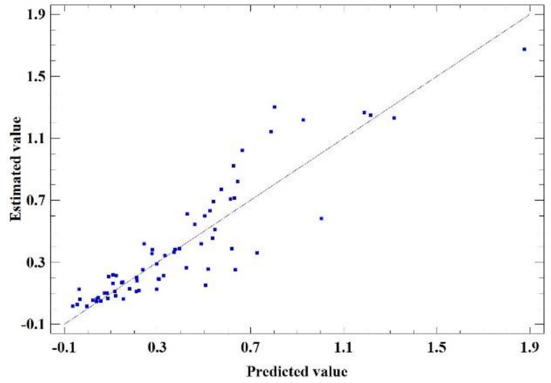


Fig. 7 Scatterplot estimated vs. predicted values of $DI_{PA,global}$ for Model 4

Table 10 Results for Model 1

| Parameter | Estimate | Standard Error | Lower Limit | Upper Limit | $P$-Value |
|---|---|---|---|---|---|
| *CONSTANT* | 0.1921 | 0.0579 | 0.0765 | 0.3077 | 0.0015 |
| *PGA/PGV* | -0.1702 | 0.0337 | -0.2376 | -0.1027 | 0.0000 |
| $I_{Arias}$ | -0.0127 | 0.0019 | -0.0166 | -0.0089 | 0.0000 |
| *SV* | -0.5529 | 0.1492 | -0.8510 | -0.2549 | 0.0004 |
| $SI_K$ | 1.7032 | 0.3172 | 1.0694 | 2.3369 | 0.0000 |
| *EPA* | 0.9300 | 0.1280 | 0.6742 | 1.1858 | 0.0000 |

Model 1 and 2 are presented in Tables 9 and 10 and their results of the analysis of variance in Tables 11 and 12, respectively.

The fitted multilinear Model 1 is presented in Eq. (30).

$$DI_{PA,global} = 0.192123 - 0.170151 \cdot PGA/PGV - 0.0127411 \cdot I_{Arias} - 0.552931 \cdot SV + 1.70315 \cdot SI_K + 0.92999 \cdot EPA \quad (30)$$

Furthermore, the fitted multilinear Model 2 is presented in Eq. (31).

$$DI_{PA,global} = -0.0862897 \cdot PGA/PGV - 0.0146593 \cdot I_{Arias} - 0.582707 \cdot SV + 1.96585 \cdot SI_K + 0.946831 \cdot EPA \quad (31)$$

### *8.2 Model 3 and 4 for the set of conventional parameters as IVs with constant*

According to the same training sample the best constructed statistical models for the set of new parameters as IVs, contain a subset of 4 parameters as explanatory variables of the equation. Model 3 and 4 are the best fitting models with and without a constant term, respectively.

The fitted multilinear Model 3 is presented in Eq. (32).

$$DI_{PA,global} = 0.0629837 + 0.064319 \cdot V_{HHT} - 0.00129891 \cdot S_{Pos,HHT} - 0.0176613 \cdot VA_{dif,HHT} + 6.51428 \cdot A_{Pos,HHT} \quad (32)$$

Furthermore, the fitted multilinear Model 4 is presented in Eq. (33).

$$DI_{PA,global} = 0.0703044 \cdot V_{HHT} - 0.00101145 \cdot S_{Pos,HHT} - 0.0192978 \cdot VA_{dif,HHT} + 6.9586 \cdot A_{Pos,HHT} \quad (33)$$

The results of the best fitting Models 3 and 4 that

Table 11 Results for Model 2

| Parameter | Estimate | Standard Error | Lower Limit | Upper Limit | *P*-Value |
|---|---|---|---|---|---|
| *PGA/PGV* | -0.0863 | 0.0241 | -0.1343 | -0.0383 | 0.0006 |
| $I_{Arias}$ | -0.0147 | 0.0020 | -0.0186 | -0.0107 | 0.0000 |
| *SV* | -0.5827 | 0.1600 | -0.9022 | -0.2632 | 0.0005 |
| $SI_K$ | 1.9659 | 0.3301 | 1.3067 | 2.6250 | 0.0000 |
| *EPA* | 0.9468 | 0.1375 | 0.6723 | 1.2214 | 0.0000 |

Table 12 Analysis of variance for Model 1

| Source | Sum of Squares | Df | Mean Square | *F*-Ratio | *P*-Value | $R^2$ (%) | $R^2$-Adjusted (%) | SEE | MAE |
|---|---|---|---|---|---|---|---|---|---|
| Model | 8.4300 | 5 | 1.686 | 58.19 | 0 | 81.9681 | 80.5594 | 0.1702 | 0.1217 |
| Residual | 1.85448 | 64 | 0.0290 | | | | | | |
| Total | 10.2845 | 69 | | | | | | | |

Table 13 Analysis of variance for Model 2

| Source | Sum of Squares | Df | Mean Square | *F*-Ratio | *P*-Value | $R^2$ (%) | $R^2$-Adjusted (%) | SEE | MAE |
|---|---|---|---|---|---|---|---|---|---|
| Model | 19.0686 | 5 | 3.8137 | 114.03 | 0 | 89.7659 | 89.1361 | 0.1829 | 0.1263 |
| Residual | 2.17399 | 65 | 0.0334 | | | | | | |
| Total | 21.2426 | 70 | | | | | | | |

describe the relationship between $DI_{PA,global}$ and 4 new proposed independent variables, with and without a constant term, are presented in Tables 13 and 14, respectively. In Tables 15 and 16 are presented the results of their variance analysis.

### *8.3 Multiple regression models quantities and results*

The results present the 95% confidence intervals for the coefficients in the multilinear model and the estimated standard error. Each variable coefficient in a model is interpreted as the mean change in the response variable based on a one-unit change in the corresponding explanatory variable keeping all other variables fixed. Of course, this interpretation of the statistical analysis is fictitious because it is not possible in a seismic excitation to change only one of the seismic parameters.

In addition, the comparison between coefficients of different explanatory variables, even in the same model, is not possible because their assigned quantities have different dimensions and units. Furthermore, all the independent variables in every multiple linear regression model are selected by the aforementioned statistical procedure primarily to predict the numerical value of the damage indicator and not to explain it physically. The constant term has a physical meaning only in the case in which all of the explanatory variables can simultaneously have zero values. Otherwise, as in the present study, the constant term is a value without physical meaning.

The *p*-value for each coefficient tests the null hypothesis that the coefficient is equal to zero (no effect). A low *p*-value (<0.05) indicates that the null hypothesis is rejected. In other words, a predictor that has a low *p*-value is likely to be a meaningful addition to the constructed model because

Table 14 Results for Model 3

| Parameter | Estimate | Standard Error | Lower Limit | Upper Limit | *P*-Value |
|---|---|---|---|---|---|
| *CONSTANT* | 0.0630 | 0.0448 | -0.0265 | 0.1524 | 0.1645 |
| $V_{HHT}$ | 0.0643 | 0.0075 | 0.0493 | 0.0793 | 0.0000 |
| $S_{Pos,HHT}$ | -0.0013 | 0.0004 | -0.0020 | -0.0006 | 0.0007 |
| $VA_{dif,HHT}$ | -0.0177 | 0.0019 | -0.0215 | -0.0138 | 0.0000 |
| $A_{Pos,HHT}$ | 6.5143 | 0.5829 | 5.3502 | 7.6783 | 0.0000 |

Table 15 Results for Model 4

| Parameter | Estimate | Standard Error | Lower Limit | Upper Limit | *P*-Value |
|---|---|---|---|---|---|
| $V_{HHT}$ | 0.0703 | 0.0062 | 0.0579 | 0.0828 | 0.0000 |
| $S_{Pos,HHT}$ | -0.0010 | 0.0003 | -0.0016 | -0.0004 | 0.0014 |
| $VA_{dif,HHT}$ | -0.0193 | 0.0015 | -0.0224 | -0.0162 | 0.0000 |
| $A_{Pos,HHT}$ | 6.9586 | 0.4934 | 5.9736 | 7.9437 | 0.0000 |

Table 16 Analysis of variance for Model 3

| Source | Sum of Squares | Df | Mean Square | *F*-Ratio | *P*-Value | $R^2$ (%) | $R^2$-Adjusted (%) | SEE | MAE |
|---|---|---|---|---|---|---|---|---|---|
| Model | 8.4497 | 4 | 2.1124 | 74.84 | 0 | 82.1602 | 81.0623 | 0.1680 | 0.1141 |
| Residual | 1.8347 | 65 | 0.0282 | | | | | | |
| Total | 10.2845 | 69 | | | | | | | |

Table 17 Analysis of variance for Model 4

| Source | Sum of Squares | Df | Mean Square | *F*-Ratio | *P*-Value | $R^2$ (%) | $R^2$-Adjusted (%) | SEE | MAE |
|---|---|---|---|---|---|---|---|---|---|
| Model | 19.3521 | 4 | 4.8380 | 168.9 | 0 | 91.1003 | 90.6957 | 0.1692 | 0.1166 |
| Residual | 1.8905 | 66 | 0.0286 | | | | | | |
| Total | 21.2426 | 70 | | | | | | | |

changes in the predictor's value are related to changes in the response variable. Conversely, a higher (insignificant) *p*-value suggests that changes in the predictor are not associated with changes in the response. Therefore, predictors with *p*-value higher than 0.05 can be dropped out without significantly degrading the constructed model.

In the analysis of variance (Tables 12-13, 16-17), the *F*-ratio value is the fraction of the model mean square divided by error mean square, and Df is the degrees of freedom for total cases, the model and their residual (for Models 1, 3: Total Df=sample size-1, Model Df=number of IVs and Residual Df=Total Df-Model Df-1 while for Models 2, 4: Total Df=sample size, Model Df=number of IVs and Residual Df=Total Df-Model Df). *F*-ratio indicates how well the model fits the data and tests the null hypothesis when is compared with *F* critical values obtained from given *F*-Tables (Tabachnick and Fidell 2013). Consequently, anything that increases the obtained *F* increases the power. Power is increased by decreasing the error variability or increasing the sample size or by increasing differences among means in the numerator.

The coefficient of determination $R^2$ is a value (in percent) which indicates that the model as fitted explains percentage equal to this value of the variability in the dependent variable (DV) equation. Adjusted $R^2$ will always be less than or equal to $R^2$, and it balances the $R^2$ value by the number of data points and independent variables in the model. If a useful independent variable is added, the adjusted $R^2$ will increase. If a useless independent variable is added, the adjusted $R^2$ will decrease. The adjusted $R^2$ statistic is more suitable for comparing models with different numbers of independent variables.

The SEE shows the standard deviation of the residuals and the MAE is the average value of the residuals.

Scatterplots (Figs. 4-7) illustrate the results of predicted values of $DI_{PA,global}$ against estimated ones from the nonlinear dynamic analyses obtained from IDARC2D for visualization the degree of their correlation.

## 9. Model validation and results interpretation

According to the most recent recommendations (Khamis and Kepler 2010), the considered minimum sample size required for multiple regression analysis is $n \geq 20+5 \cdot m$ (where m is the number of IVs). Even though the used sample size is not quite higher from the required minimum one, all the above statistical models give a high prediction of the Park and Ang overall structural damage of the structure under study. High approximation of estimated $DI_{PA,global}$ from predicted $DI_{PA,global}$ is resulting, observing first, the Standard Error of Estimation (SEE) and the Mean Absolute Error (MAE) and then, the $R^2$ and adjusted $R^2$ of the models.

In every model, the *p*-value of the coefficients of the selected IVs-parameters is lower than 0.05. Consequently, all the coefficients in the models are significant to the prediction of the $DI_{PA,global}$.

Detecting the critical *F*-values for every regression analysis from the relevant F-Tables (Tabachnick and Fidell 2013) the values are taken 3.76 and 4.14 for Model 1-2 and 3-4, respectively. Comparing the critical *F*-values with the calculated ones (the smallest calculated is $F$=58.19) the null hypothesis is rejected and the increased power of the model is resulting.

Examining the scatterplots (Figs. 4-7) of observed and predicted values of $DI_{PA,global}$ is obvious that the predicted values display very satisfactory approximation to the real ones till the value of 0.7. Above the value of 0.7 the estimated values of $DI_{PA,global}$ are more scattered in both plots. The reason for weak significance for these values may be a result of the reduced number of motions resulting serious damage effects, in the testing sample.

The mutual comparison of the models shows that the new presented parameters offer equal and even better prediction of the $DI_{PA,global}$. Particularly the SEE and the adjusted $R^2$ of the Models 3-4 corresponding to the new parameters are from 0.1680 to 0.1692 and from 81.0623% to 90.6957%, respectively, while for Models 1-2, these values range from 0.1702 to 0.1829 and from 80.5594% to 89.1361%, respectively. From all the models the most significant according to the determined indicator “Standard Error of Estimation” or “Mean Absolute Error” seems to be Model 3 which presents the lowest one (SEE=0.1680 and MAE=0.1141).

Table 18 Prediction of $DI_{PA,global}$ and their absolute difference with the estimated ones

| Model 1 | | | |
|---|---|---|---|
| Seismic excitation | $DI_{PA,global}$ | Fitted Value | Absolute difference |
| Friuli | 0.541 | 0.452 | 0.089 |
| Central Italy | 0.056 | 0.117 | 0.061 |
| Ardal | 0.367 | 0.455 | 0.088 |
| Amberley New Zealand | 0.394 | 0.505 | 0.111 |
| Amberley New Zealand | 1.289 | 0.833 | 0.456 |
| Amberley New Zealand | 0.221 | 0.043 | 0.178 |
| Amberley New Zealand | 0.193 | 0.156 | 0.037 |
| Amberley New Zealand | 0.617 | 0.750 | 0.133 |
| Amberley New Zealand | 0.895 | 0.597 | 0.298 |
| Amberley New Zealand | 1.424 | 1.252 | 0.172 |
| Mean Absolute Difference | | | 0.162 |
| Model 2 | | | |
| Seismic excitation | $DI_{PA,global}$ | Fitted Value | Absolute difference |
| Friuli | 0.541 | 0.363 | 0.178 |
| Central Italy | 0.056 | 0.056 | 0.000 |
| Ardal | 0.367 | 0.445 | 0.078 |
| Amberley New Zealand | 0.394 | 0.458 | 0.064 |
| Amberley New Zealand | 1.289 | 0.904 | 0.385 |
| Amberley New Zealand | 0.221 | 0.061 | 0.160 |
| Amberley New Zealand | 0.193 | 0.139 | 0.054 |
| Amberley New Zealand | 0.617 | 0.732 | 0.115 |
| Amberley New Zealand | 0.895 | 0.617 | 0.278 |
| Amberley New Zealand | 1.424 | 1.315 | 0.109 |
| Mean Absolute Difference | | | 0.142 |
| Model 3 | | | |
| Seismic excitation | $DI_{PA,global}$ | Fitted Value | Absolute difference |
| Friuli | 0.541 | 0.470 | 0.071 |
| Central Italy | 0.056 | 0.066 | 0.010 |
| Ardal | 0.367 | 0.371 | 0.004 |
| Amberley New Zealand | 0.394 | 0.430 | 0.036 |
| Amberley New Zealand | 1.289 | 0.969 | 0.320 |
| Amberley New Zealand | 0.221 | 0.220 | 0.001 |
| Amberley New Zealand | 0.193 | 0.261 | 0.068 |
| Amberley New Zealand | 0.617 | 0.626 | 0.009 |
| Amberley New Zealand | 0.895 | 0.707 | 0.188 |
| Amberley New Zealand | 1.424 | 1.707 | 0.283 |

Table 18 Continued

| Mean Absolute Difference | | | 0.099 |
|---|---|---|---|
| Model 4 | | | |
| Seismic excitation | $DI_{PA,global}$ | Fitted Value | Absolute difference |
| Friuli | 0.541 | 0.453 | 0.088 |
| Central Italy | 0.056 | 0.025 | 0.031 |
| Ardal | 0.367 | 0.342 | 0.025 |
| Amberley New Zealand | 0.394 | 0.440 | 0.046 |
| Amberley New Zealand | 1.289 | 1.047 | 0.242 |
| Amberley New Zealand | 0.221 | 0.299 | 0.078 |
| Amberley New Zealand | 0.193 | 0.273 | 0.080 |
| Amberley New Zealand | 0.617 | 0.688 | 0.071 |
| Amberley New Zealand | 0.895 | 0.787 | 0.108 |
| Amberley New Zealand | 1.424 | 1.787 | 0.363 |
| Mean Absolute Difference | | | 0.113 |

For the verification of the conducted results and the quality of the models, a subset of 10 earthquake velocity time series is used as a set of validation data and a blind prediction of the $DI_{PA,global}$ occurs. Applying the models to the sets of the estimated parameters for these 10 seismic excitations, the value of Park-Ang damage indices of the structure in the study, caused by the subset of earthquakes, is calculated in STATGRAPHICS. The results presented in Table 18.

From the mean absolute difference between the estimated $DI_{PA,global}$ and the predicted ones from the equations of the models, best results seem to come of the new parameters end the best model of all is resulting in being Model 3 as the estimated indicators revealed.

## 10. Conclusions

Nonstationary and nonlinear seismic signals are analyzed using the HHT analysis procedure. The results are presented in time-frequency-amplitude space, and the Hilbert spectrum is obtained. Physical and geometric features of the Hilbert spectrum are connected with seismic features and considered as new intensity parameters.

The usefulness and the effectiveness of the new seismic parameters proposed in this study are validated exemplary by two statistical procedures. The first one is a correlation analysis and the second one is a multiple linear regression analysis. The aim is to verify that the new proposed seismic intensity parameters have the same or even better results in the above statistical applications in comparison with the conventional ones. For this reason, a set of conventional parameters are extracted from the accelerograms employed. Beside them, novel parameters are proposed and evaluated by numerical processing of the seismic velocity time histories of the utilized corresponding acceleration records using the HHT analysis technique. The overall damage index of Park and Ang is used to describe the damage of a seven-story reinforced concrete frame structure under seismic excitation. Observing the well-known and already proved interdependence between the conventional seismic parameters and using the correlation analysis, a similar association between the proposed new parameters and the structural post seismic damage grade is conducted.

The statistical method of multilinear regression analysis is used to predict the damage of the reinforced concrete frame from the set of conventional parameters and the set of the proposed new parameters separately. The results of predicted (by multiple linear regression) and estimated (by nonlinear dynamic analyses) overall damage indices for a subset of 70 excitations are compared. A very satisfactory prediction of the Park and Ang overall damage index is achieved which seems to be even more accurate using the new parameters derived from the estimated Hilbert spectrum of every seismic signal.

Finally, a subset of the rest 10 seismic excitations is used to verify (by blind prediction) the fitted models produced from the regression analysis. The results confirm the fidelity of the damage prediction accomplished from the here novel proposed parameters which are presented to be of equivalent and better quality from this accomplished from a set of conventional parameters.

## References


Alvanitopoulos, P., Andreadis, I. and Elenas, A. (2010), "Interdependence between damage indices and ground motion parameters based on Hilbert-Huang transform", *Measur. Sci. Technol.*, **21**(2), 025101-025115.

Alvanitopoulos, P., Papavasileiou, M., Andreadis, I. and Elenas, A. (2012), "Seismic intensity feature construction based on the Hilbert-Huang transform", *IEEE Tran. Instrum. Measur.*, **61**(2), 326-337.

Araya, R. and Saragoni, G.R. (1984), "Earthquake accelerogram destructiveness potential factor", *Proceedings of the 8th World Conference on Earthquake Engineering*, EERI, El Cerrito, CA, USA.

Arias, A. (1970), "A measure of earthquake intensity", *Seismic Design for Nuclear Power Plants*, Ed. Hansen, R.J., MIT Press, Cambridge, MA, USA.

ATC 3-06 Publication (1978), Tentative Provisions for the Development of Seismic Regulations for Buildings, US Government Printing Office, Washington, DC, USA.

Battista, B.M., Knapp, C.C., McGee, T. and Goe bel, V. (2007), "Application of the empirical mode decomposition and Hilbert-Huang transform to seismic reflection data", *Geophys.*, **72**(2), H29- H37.

Cabãnas, L., Benito, B. and Herráiz, M. (1997), "An approach to the measurement of the potential structural damage of earthquake ground motions", *Earthq. Eng. Struct. Dyn.*, **26**(1), 79-92.

Chopra, A.K. (1995), *Dynamics of Structures*, Prentice-Hall, Englewood Cliffs, NJ, USA.

EC2 (2000), Eurocode 2: Design of Concrete Structures—Part 1: General Rules and Rules for Buildings, European Committee for Standardization, Brussels, Belgium.

EC8 (2004), Eurocode 8: Design of Structures for Earthquake Resistance-Part 1: General Rules, Seismic Actions, and Rules for Buildings, European Committee for Standardization, Brussels, Belgium.

Elenas, A. (1997), “Interdependency between seismic acceleration parameters and the behavior of structures”, *Soil Dyn. Earthq. Eng.*, **16**(5), 317-322.
Elenas, A. (2000), “Correlation between seismic acceleration parameters and overall structural damage indices of buildings”, *Soil Dyn. Earthq. Eng.*, **20**(1), 93-100.
Elenas, A. (2014), “Seismic-parameter-based statistical procedure for the approximate assessment of structural damage”, *Math. Prob. Eng.*, **2014**, Article ID 916820.
Elenas, A. and Meskouris, K. (2001), “Correlation study between seismic acceleration parameters and damage indices of structures”, *Eng. Struct.*, **23**(6), 698-704.
Elenas, A., Liolios, A. and Vasiliadis, L. (1995), “Earthquake-induced nonlinear behavior of structures interrelation with characteristic acceleration parameters”, *Proceedings of the 10th European Conference on Earthquake Engineering*, Vienna, 1011-1016.
Ercan, I., Mehmet, F.I. and Mehmet, A.B. (2017), “Web-based evaluation of earthquake damages for reinforced concrete buildings”, *Earthq. Struct.*, **13**(4), 387-396.
Fajfar, P., Vidic, T. and Fischinger, M. (1990), “A measure of earthquake motion capacity to damage medium-period structures”, *Soil Dyn. Earthq. Eng.*, **9**(5), 236-242.
Gholamreza, G.A. and Elham, R. (2018), “Maximum damage prediction for regular reinforced concrete frames under consecutive earthquakes”, *Earthq. Struct.*, **14**(2), 129-142.
Housner, G.W. (1952), “Spectrum intensities of strong-motion earthquakes”, *Proceedings of the Symposium on Earthquake and Blast Effects on Structures*, EERI, Oakland, CA, USA.
Huang, N., Shen, Z., Long, S.R., Wu, M.C., Shih, H.H., Zheng, Q., Yen, N.C., Tung, C. and Liu, H. (1998), “The empirical mode decomposition and the Hilbert spectrum for nonlinear and non-stationary time series analysis”, *Proceedings of the Royal Society of London A, Math. Phys. Eng. Sci.*, **454**, 903-995.
Huang, N., Wu, M.L., Qu, W., Long, S. and Shen, S. (2003), “Applications of Hilbert-Huang transform to non-stationary financial time series analysis applied stochastic models in business and industry”, *Appl. Stoch. Model. Business Ind.*, **19**(3), 245-268.
Huang. N., Shen, Z. and Long, S.R. (1999), “A new view of nonlinear water waves: The Hilbert spectrum”, *Annu. Rev. Fluid Mech.*, **31**(1), 417-457.
Husid, R.L. (1969), “Analisis de terremotos: analisis general”, *Revista del IDEM*, **8**(1), 21-42.
Jennings, P.C. (1982), “Engineering seismology”, *Earthquakes: Observation, Theory and Interpretation*, Eds. Kanamori, H. and Boschi, E., Italian Physical Society, Varenna, Italy.
Kappos, A.J. (1990), “Sensitivity of calculated inelastic seismic response to input motion characteristics”, *Proceedings of the 4th U.S. National Conference on Earthquake Engineering*, EERI, Oakland, CA, USA.
Khamis, H.J. and Kepler, M. (2010), “Sample size in multiple regression: 20+5k”, *J. Appl. Stat. Sci.*, **17**(4), 505-517.
Kostinakis, K. (2018), “Impact of the masonry infills on the correlation between seismic intensity measures and damage of R/C buildings”, *Earthq. Struct.*, **14**(1), 55-71.
Kostinakis, K. and Morfidis, K. (2017), “The impact of successive earthquakes on the seismic damage of multistorey 3D R/C buildings”, *Earthq. Struct.*, **12**(1), 1-12.
Martinez-Rueda, J.E. (1998), “Scaling procedure for natural accelerograms based on a system of spectrum intensity scales”, *Earthq.e Spectra*, **14**(1), 135-152.
Meskouris, K. (2000), *Structural Dynamics: Models, Methods, Examples*, Ernst & Sohn, Berlin, Germany.
Meskouris, K., Krätzig, W.B. and Hanskötter, U. (1993), “Nonlinear computer simulations of seismically excited wall-stiffened reinforced concrete buildings”, *Proceedings of the 2nd International Conference on Structural Dynamics (EURODYN ’93)*, Balkema, Lisse, The Netherlands.
Nanos, N., Elenas, A. and Ponterosso, P. (2008), “Correlation of different strong motion duration parameters and damage indicators of reinforced concrete structures”, *Proceedings of the14th World Conference on Earthquake Engineering*, Beijing, China.
Park, Y.J. and Ang, A.H.S. (1985), “Mechanistic seismic damage model for reinforced concrete”, *J. Struct. Eng.*, **111**(4), 722-739.
Park, Y.J., Ang, A.H.S. and Wen, Y.K. (1987), “Damage-limiting aseismic design of buildings”, *Earthq. Spectra*, **3**(1), 1-26.
Pejovic, J.R., Serdar, N.N. and Pejovic, R. (2017), “Optimal intensity measures for probabilistic seismic demand models of RC high-rise buildings”, *Earthq. Struct.*, **13**(3), 221-230.
Reinhorn, A.M., Roh, H., Sivaselvan M. *et al*. (2009), “IDARC2D version 7.0: a program for the inelastic damage analysis of structures”, Tech. Rep., MCEER-09-0006, MCEER, State University of New York at Buffalo, New York, NY, USA.
Statpoint Technologies Inc. (2016), STATGRAPHICS Centurion XVII User Manual, StatPoint, Herndon, VA, USA.
Tabachnick, B.G. and Fidell, L.S. (2013), *Using Multivariate Statistics*, 6th Edition, Pearson Education Inc., Upper Saddle River, NJ, USA.
Trifunac, M.D. and Brady, A.G. (1975), “A study on the duration of strong earthquake ground motion”, *Bull. Seismol. Soc. Am.*, **65**(3), 581-626.
Uang, C.M. and Bertero, V.V. (1990), “Evaluation of seismic energy in structures”, *Earthq. Eng. Struct. Dyn.*, **19**(1), 77-90.
Vanmarcke, E.H. and Lai, S.S.P. (1980), “Strong-motion duration and RMS amplitude of earthquake records”, *Bull. Seismol. Soc. Am.*, **70**(4), 1293-1307.
Vrochidou, E., Alvanitopoulos, P., Andreadis, I. and Elenas, A. (2016), “Structural damage estimation in mid-rise reinforced concrete structure based on time-frequency analysis of seismic accelerograms”, *IET Sci. Measur. Technol.*, **10**(8), 900-909.
Vrochidou, E., Alvanitopoulos, P., Andreadis, I. and Elenas, A. (2018), “Artificial accelerograms composition based on the CEEMD”, *Tran. Inst. Measur. Control*, **40**(1), 239-250.
Vui, V.C. and Hamid, R.R. (2014), “Correlation between parameters of pulse-type motions and damage of low-rise RC frames”, *Earthq. Struct.*, **7**(3), 365-384.
Yan, R.Q. and Gao, R.X. (2007), “A tour of the tour of the Hilbert-Huang transform: An empirical tool for signal analysis”, *IEEE Instrum. Meas.Mag.*, **10**(5), 40-45.
Zhang, R.R., Ma, S., Safak, E. and Hartzell S. (2003), “Hilbert-Huang transform analysis of dynamic and earthquake motion recordings”, *J. Eng. Mech.*, ASCE, **129**(8), 861-875.

*AT*